Assessment and Ranking of the Severity of Disturbances in the Mexican Interconnected System

J.M. Ramos-Guerrero*, M.R.A. Paternina*, F. R. Segundo Sevilla†, A. Obusevs †, J.A. Moreno-Corbea*, D. Rodales‡, A. Sánchez§, A. Zamora‡ and J.M. Ramírez§
*UNAM, Mexico City, †ZHAW, Winterthur, Switzerland, ‡U. Michoacana, Morelia, Mexico, §CINVESTAV, Guadalajara, Mexico

***Abstract*—This paper adopts a methodology to assess and rank the severity of the most frequent disturbances, 3 types in particular, that occur in the Mexican Interconnected System (MIS) when wind power plants (WPPs) are integrated. This is done by combining three stability indices from which an overall performance measure can be derived. In this way, it is possible to assess the severity of the disturbances such as generation tripping, line tripping and disconnection of loads. The indices under consideration include measures such as maximum amplitude, speed variation, and the Lyapunov exponent. For ranking the severity, a general index value is used. To confirm the effectiveness and performance of the proposed methodology, this paper investigates the 190-bus and 46-generator MIS equipped with an 8% of wind generation to quantitatively evaluate the severity of disturbances, resulting in 66% of unstable disturbances which are associated with the disconnection of loads.**

***Index Terms*—Ranking of severity, disturbances analysis, Lyapunov exponent, rate-of-change-of-frequency, maximum amplitude.**

I. Introduction

A. Motivation

The accelerated growth of renewable energy sources (RESs) together with the necessity to meet low carbon emissions are two key goals of the Mexican government. In this transition, Mexico has reached about 17 % of solar and wind energy in 2023, imposing challenges for the operation and control of the Mexican Interconnected System (MIS). A part of these challenges is mainly unleashed by different types of disturbances that expose the system's security. Thus, knowing the severity of such disturbances can enhance the decision-making process at the control centers that monitor the system taking advantage of the deployment of wide-area infrastructure [1].

B. State-of-the-art

The advent of RESs has degraded the power system transient stability, which is evidenced when large disturbances take place across power grids [2]. Thus, it is relevant to quantify this impact by introducing the concept of power system flexibility, consisting of the ability in retaining the balance between load and generation in the presence of disturbances [3]. Such flexibility is affected due to the intermittency and drawbacks to forecasting the behavior of RESs [4], which has led to investigate the quantification of this impact [5]. For instance, in [6] the transient stability analysis incorporating the intermittency and volatility of the wind resource is tackled to evaluate the stability in the presence of wind power plants equipped with DFIGs and PMSGs.

According to the power system literature [7], [8], the evaluation of transient stability is conveyed by indices that determine if the system is stable or unstable after disturbances take place. In [9], [10], a collection of stability indices shows that the angle and rotor angle speed variables of synchronous generators are widely used, resulting in up to 13 stability indices, and being the most used those associated with the rotor angle of synchronous machines. For instance, authors in [11] have proposed the angle stability limit that evaluates the relationship between active power and rotor angle to different contingencies, yielding a region that indicates the stability limits per magnitude. In [12], the critical clearing time (CCT) index is used to determine the maximum time to clear a fault and a stable region that is bounded and defined when the clearing time is greater than the CCT. Likewise, authors in [13], [14] employ the Lyapunov exponent (LE) to rank the severity of large events in the system.

Lyapunov exponents have been used to evaluate the chaos to different initial conditions [15]. For instance, the maximum Lyapunov exponent (MLE) has been used for cancer early detection [16]. The computation of LEs can be implemented according to the nature of the analyzed signal and the wished accuracy. In [17], [18], authors have demonstrated that the computation of LEs in discrete time is suitable when projections onto the linear system are involved, requiring less computational effort and drawing reliable results.

In power system literature, the LEs have been introduced to assess the transient stability under the massive penetration of wind power plants [19]. They exhibit how the stability of the system is degraded when the percentage of renewable energy integration is increased. Also, the authors prove that the loss of inertia contributes to the stability's degradation. In [20], the LEs are used to find the optimal bus for integrating distributed energy resources (DERs) by computing the MLE from phasor voltage signals and selecting the negative values with a higher amplitude among a set of buses. Authors in [21] have performed real-time rotor angle stability analysis by considering a discrete formulation and analyzing the signals' divergence to large disturbances.

C. Problem statement

In Mexico, the renewable energy integration of solar and wind has reached 17 % of the total installed capacity in 2023 [22], which has unleashed unexpected operational scenarios that have led to the sudden disconnection of solar and wind power plants. This fact together with the lack of analysis tools motivates us to investigate the severity of different disturbances across the Mexican power system.

D. Contribution

The main contribution of this investigation lies in adopting a methodology to assess and rank the disturbances' severity in the Mexican power grid. To validate and confirm the proposal, different disturbances are simulated in the Mexican interconnected power system including wind power plants (WPPs). This methodology allows to sort of all disturbances from the less up to the most severe, by using three stability indices: (*i*) Lyapunov exponent that allows to know the system recovering capacity; (*ii*) speed variation enables to track fast and sudden changes; and (*iii*) the oscillation's amplitude for fulfilling the grid codes [23]. Likewise, a general performance index that meets and provides a specific contribution by assigning weight factors to each stability index, is used. To carry out our proposal, the Power System Toolbox in [24], [25] is used to run transient stability simulations on the Mexican interconnected grid by implementing generation, line, and load trips.

E. Organization

The remaining sections of the paper are structured as follows. The fundamentals and their straightforward algorithmic implementations adopted to compute the severity indices are enclosed in Section II. The proposed methodology to assess and rank the disturbances' severity is exposed in Section III. Multimachine simulations and test cases are exhibited in Section IV. The assessment and ranking of disturbances' severity are carried out in Section V. Finally, concluding remarks are described in Section VI.

II. Indices of Severity

The severity of grid disturbances on large-scale power systems can be evaluated and ranked by indices such as the Lyapunov exponent or other indices such as maximum amplitude and speed variation [14]. These indices are described in the following.

A. Maximum Amplitude

This index is computed to ensure the grid codes' compliance. It uses a normalized value of the maximum amplitude corresponding to the measurement during or after the disturbance takes place, as follows:

$$\lambda_{am} = \frac{\sum_{i=1}^{n} max(|f_0 - min(f_i)|, |f_0 - max(f_i)|)}{n} \quad (1)$$

where n stands for the total number of buses, f_0 indicates the fundamental frequency of the system, f_i corresponds to the frequency at the i-th bus.

B. Speed Variation

Since the fast transients are detrimental to global stability and synchronism, this index is applied to the rotor speed oscillations of large-scale generators. The maximum rotor speed deviation is reached by the generator during or after the fault [13].

$$RoCoF_i = \sum_{i=1}^{M} \frac{f_i - f_{i-1}}{\triangle t} \quad (2)$$

$$\lambda_{de} = \frac{\sum_{i=1}^{n} max(RoCoF_i)}{n} \quad (3)$$

where f_i is the frequency at the current sample, M is the total number of samples and f_{i-1} is the frequency at the previous sample that is spaced by the step size (Δt).

C. Lyapunov Exponent

Several approaches can be chosen to evaluate the stability problem with renewable energy [26]. One of them is to evaluate a measurable trajectory, according to how it evolves over time depending on its initial conditions. To this end, the Lyapunov exponents are commonly used due to they allow to evaluate such trajectories from an equilibrium point and to determine whether the trajectory is chaotic or not depending on the resulting sign. A positive exponent indicates that the trajectory is chaotic in time (it is an unstable trajectory), whereas a negative exponent indicates that the trajectory tends to converge to a point (it is a stable trajectory) [23]. In power systems, the short-term stability can be analyzed starting from an equilibrium point in steady state. Therefore, the Lyapunov exponent is a good indicator to determine transient stability [27].

Lyapunov exponents are conventionally computed for dynamic systems in the form [28]:

$$\dot{x} = F(x) \quad (4)$$

whose solution is assumed as $f^t(x)$. Now, if two initial conditions are considered such as x_0 and $x_0 + \delta x_0$, being δx_0 a small perturbation around x_0; then after a time period t, the solutions for each initial condition are given by $f^t(x_0)$ and $f^t(x_0 + \delta x_0)$, respectively, establishing two trajectories. Thus, the separation among these trajectories can be defined by $\Delta f^t = f^t(x_0 + \delta x_0) - f^t(x_0)$, indicating divergence or convergence, and in turn if the system is unstable or stable, respectively. When one of the trajectories behaves chaotically, then the separation Δf^t erratically varies in time, being necessary to introduce an exponential measured rate to quantify such separation among trajectories which can be expressed as:

$$\lambda = \lim_{t \to \infty} ln |\frac{\triangle f^t}{\delta x_0}| \quad (5)$$

where λ is the Lyapunov exponent and δx_0 is assumed that tends to zero. If f^t is linearized, it satisfies:

$$\Delta f^t = f^t(x_0 + \delta x_0) - f^t(x_0) = D_{x_0} f^t(x_0) \delta x_0 \quad (6)$$

where D_{x_0} symbolizes the partial derivative $\partial f / \partial x_0$. Thus, (5) can be rewritten as:

$$\lambda = \lim_{t \to \infty} \frac{|D_{x_0} f^t(x_0) \delta x_0|}{|\delta x_0|} \quad (7)$$

Notice that the term δx_0 represents the initial separation, which contains any component in the direction associated with the maximum Lyapunov exponent. Given the exponential growth of the Lyapunov exponent, the effect over other exponents is attenuated until vanishing in time.

According to [13], [29], the application of the Lyapunov exponents in power systems can be implemented to analyze voltage and frequency signals. Thus, for the frequency, we have:

$$LE^m = \frac{1}{N \triangle t} \sum_{m=1}^{N} log_{10}(\frac{|f^n_{k+m} - f^n_{k+m-1}|}{|f^n_m - f^n_{m-1}|}) \quad (8)$$

To perform the evaluation of the Lyapunov exponent, a strategy with sliding windows is used to analyze the frequency signals and to compare the exponent with the steady state condition before the disturbance occurs. This strategy is exhibited in Fig. 1, where the length of the window starts at the instant $d+N$, being N the instant where the frequency signal has the second peak after the disturbance takes place, and d is the instant after the frequency signal is out of the frequency limits. Then, the LE is computed until the instant $M-N-d$.

For the n-th bus, a LE average can be calculated as [13]:

$$\alpha^n_{le} = \frac{\sum_{m=N+d}^{M-N-d} LE^m}{M - 2N - 2d} \quad (9)$$

Finally, the global Lyapunov exponent index for the whole power grid is computed as:

$$\lambda_{le} = \frac{\sum_{i=1}^{n} \alpha^n_{le}}{n} \quad (10)$$

D. General performance index

Once all indices have been computed, the general performance index (λ_g) allows to rank the severity of the disturbance. This is computed by:

$$\lambda_g = \lambda_{am} * \omega_{am} + \lambda_{de} * \omega_{de} + \lambda_{le} * \omega_{le} \quad (11)$$

where $\omega_{am} = 25$, $\omega_{de} = 1$ and $\omega_{le} = 50/35$ are weight factors that respectively correspond to each index.

III. Methodology for Ranking Severity

To rank the disturbances' severity, the methodology in Fig. 2 is stated in three stages. This allows obtaining a general performance index to determine the stability grade, sorting the disturbances' severity from the less relevant to the most critical. Each stage is described in the following. The first stage is presented in the gray square in Fig. 2, it consists in preparing multi-machine transient simulations in the power system toolbox (PST) [24], [25] to obtain frequency signals that are stored in a phasor data concentrator (PDC). The frequency computation is implemented according to the Std. IEEE C37.118.1, where it is conceived as the first derivative of the phase angle, as follows [30], [31]:

$$f(t) = f_0 + \Delta f(t), \quad (12)$$

where f_0 is the fundamental frequency and $\Delta f(t)$ is the deviation of frequency from nominal given by

$$\Delta f(t) = \frac{1}{2\pi} \left[\frac{\hat{\varphi}_{a1,k} - \hat{\varphi}_{a1,k-1}}{\Delta t} \right], \quad (13)$$

where $\hat{\varphi}$ is the positive-sequence phasor angle, k indicates the actual iteration processed in the simulation, and $\Delta(t)$ corresponds to the window time between each synchrophasor estimated.

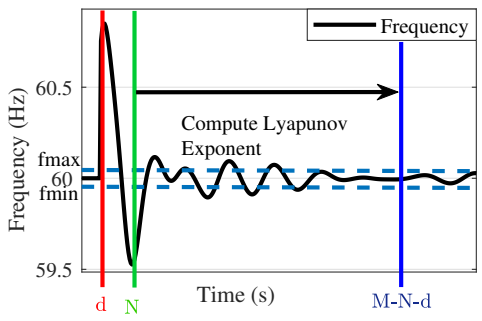

Fig. 1: Sliding window strategy for computing the Lyapunov exponents.

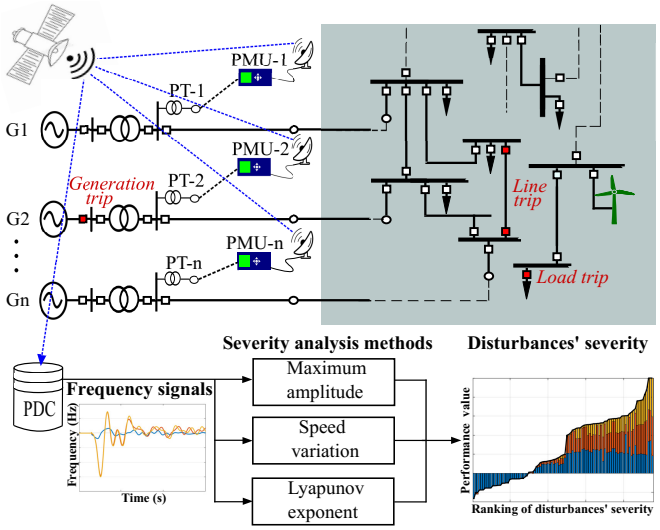

Fig. 2: Methodology for assessing and ranking the disturbances' severity in the Mexican system.

The second stage is shown at the bottom of Fig. 2, it deals with the indices' computation such as maximum amplitude, speed variation and Lyapunov exponent via (1)-(10) in Section II.

Finally, the evaluation of the ranking severity is performed in the third stage by obtaining a general performance index that uses the information provided by all three indices that quantify the disturbances' severity, as shown in Fig. 2.

The whole evaluation is conveyed by implementing the **Algorithm 1** to assess and rank the disturbances' severity. This algorithm requires a set of n time-series data of recorded frequency signals f with M samples, the nominal frequency f_0, and the minimum f_{min} and maximum f_{max} frequency thresholds established by the grid code; for the Mexican system, these limits are defined as $f_0 = \pm 0.01$ Hz. This set is used as input to compute all three severity indices. For the maximum amplitude index, the signals are analyzed by finding the maximum value either positive or negative of the frequency signals normalized by the fundamental frequency, as shown in (1). For the speed variation index, all signals are processed sample by sample, as indicated in (2)-(3), where a sampling rate of 60 Hz is used. For the Lyapunov exponent, all signals are analyzed by (8), where it is necessary to detect when the frequency signals are out of the band between the minimum f_{min} and maximum frequency f_{max}, then the second peak after the disturbance is detected to establish N, aiming to determine the length of the analysis window. When all the Lyapunov exponents are computed, they are averaged by (9). Once all indices are computed, the ranking of severity is defined by applying weight factors to the indices, as shown in (11), which enables the sorting of all disturbances.

IV. Simulation Environment and Test Case: Mexican Interconnected System

This section simulates a reduced version of the Mexican interconnected system in PST [24], [25]. All simulations consist of a total simulation time of 20s, disturbance inception at 1s, lasting 50 ms, and a sampling frequency of 60 Hz. The MIS is assessed under generation trips, line outages and loss of load, deriving three cases C1, C2 and C3, respectively. The cases for generation trip (*C1*), line outages (*C2*), and loss of load (*C3*) are conducted by modifying the switching data in *sw_con* to define the buses associated with those elements. Finally, a trip is accomplished on the line that directly connects the generation or line to be disconnected.

In any case, the reading of these functions is contained in *s_simu*; the *s_simu* function calls the PST models for data file selection, load

Algorithm 1 Computation of the disturbances' severity and ranking.

Inputs:
A set of n time-series data of recorded signal $f(n,M)$ with M samples each. The minimum and maximum frequency limits in steady-state f_{min} and f_{max}, respectively. The fundamental frequency f_o.
Output: Ranking of severity λ_g
while $i <= n$ **do**
  Initialization: $d=1$, $j=1$, $h=1$, $\alpha=0$ and $l_e=0$
  To compute the maximum amplitude:
  $\lambda_{am} = \max[abs(f_0 - min(f(i,:))), abs(f_0 - max(f(i,:)))]$
  To compute the speed variation:
  $\lambda_{de} = \max(f(i,2:l) - f(i,1:l-1)/\triangle t)$
  while j==1 **do**
    if $f(i,d) >= f_{min}$ & $f(i,d) <= f_{max}$) **then**
      d=d++
      ELSE
      j==2
      N=d
    end if
  end while
  while h=1 **do**
    if $f(i,N) > f_{max}$ & $f(i,N-1) > f(i,N)$ ||
    $f(i,N) < f_{min}$ & $f(i,N-1) < f(i,N)$ **then**
      N=N++
      p=p++
      ELSE
      h==2
    end if
  end while
  To compute the Lyapunov Exponent:
  for $k = (N+d) : (M-N-d)$ **do**
    for $m = 1 : N-d$ **do**
      $$l_e = l_e + log_{10}\left(\frac{abs(f(i,k+m) - f(i,k+m-1))}{abs(f(i,m) - f(i,m-1))}\right)$$
    end for
  end for
  To compute the Lyapunov exponent's average
  $LE(i,k) = l_e/(N \times \triangle t)$
  for p=(N+d):(M-N-d) **do**
    $\alpha = LE(i,p) + \alpha$
  end for
  $\lambda_{le} = \alpha/(M-2N-2d)$
  i=i++
end while
To compute the ranking of severity:
$\lambda_g = \lambda_{am} * \omega_{am} + \lambda_{de} * \omega_{de} + \lambda_{le} * \omega_{le}$

flow development and solution, initialization of the nonlinear simulation models, and step-by-step integration of the dynamic equations to respond to a user-specified system fault, following the procedure in [25].

The 190-bus and 46-synchronous machine MIS shown in Fig. 3 is selected as a test system. It contains 46 synchronous generators, 7 wind power plants, 143 loads, 217 transmission lines, and 48 transformers. The MIS represents a simplified model of the Mexican transmission system, whose nominal frequency is 60 Hz and the main grid voltage is 400 kV (rated voltage) [22], [32], [33].

In Mexico, there are four electrical systems that operate in isolation, Muleje, Baja California (BCA), Baja California Sur (BCS), and the MIS which is the largest one. The total installed capacity is approximately 83,120MW with a maximum demand about 50GW in 2019. The BCA system is interconnected to the California ISO (CAISO) through two synchronous 230kV transmission lines (TL). Meanwhile, the MIS is a mesh system with radial connections towards the northwest and southeast. Its transmission level is mainly composed of TLs with operating voltages of 400kV, 230 kV and 130-69kV. This system covers from Quintana Roo to Sonora state, making up the main electrical power grid in Mexico, and it is split into 7 regions: Central, Eastern, Western, Northwestern, North, Northeastern, and Peninsular. It also has six trade international interconnections: (*i*) there are four asynchronous connections in the Northeastern region with the Electric Reliability Council of Texas (ERCOT) in USA by four tie-lines with 436MW capacity; (*ii*) there is one synchronous connection in the Eastern region with Guatemala via one tie-line with 240MW capacity;

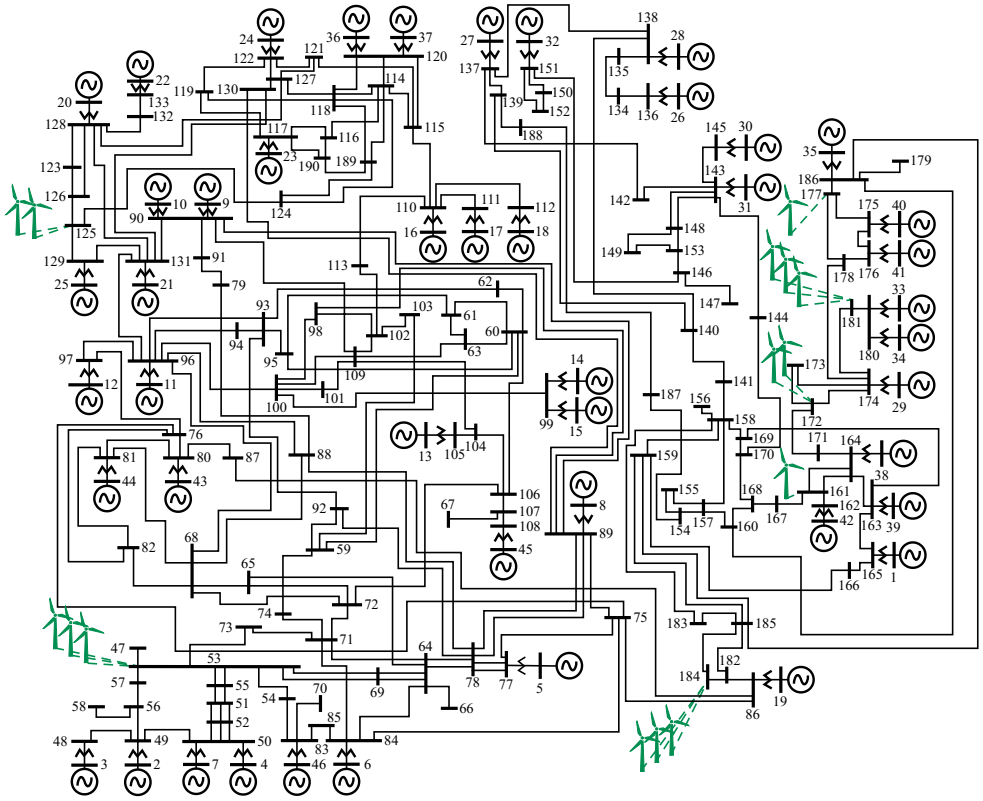

Fig. 3: Single-line diagram of the 190-bus and 46-machine Mexican power system with 8% of wind penetration.

and (*iii*) there is also one synchronous connection in the Peninsular region with Belize by one tie-line with 55MW capacity. For the sake of brevity, public official documents are available at [22]. To generate the Mexican grid disturbances' library, test cases related to the generation, line, and load trips are simulated considering the following.

A. Generator trips

For the evaluation of the severity of generation trips, it was chosen to evaluate each one of the 46 generators in the MIS. To this end, each of the generation buses was disconnected to determine in which region the greatest severity would be applied in order to obtain compatible buses for the connection of wind power plants near the generation points.

B. Line trips

For the selection of the transmission lines to be evaluated, it is determined to choose those with power flows greater than 300 MW, representing a total of 33 out of the 217 lines of the MIS. For each of them, a disconnection is simulated.

C. Load trips

Loads greater than 200 MVA are selected, since they represent the largest cities in the country, and the severity of the sudden disconnection of these loads is evaluated to investigate the indices variation under critical scenarios. A total of 16-load disconnection is evaluated.

V. Assessment and Ranking of Disturbances' Severity in MIS

The severity evaluation is carried out in two cases of the MIS: (*i*) Without wind generation and (*ii*) with an 8% of wind generation. The same disturbances are evaluated for each case. The attained results are exhibited in Figs. 4 and 5. The behavior of the three indices is shown together with the index value that is computed after normalizing and considering weighting factors. Thus, the disturbances' severity is ranked following that the less severe disturbance corresponds to the less negative value; meanwhile, the most severe disturbance is associated with the greater positive value, thereby all disturbances are sorted from the less up to the greatest severity.

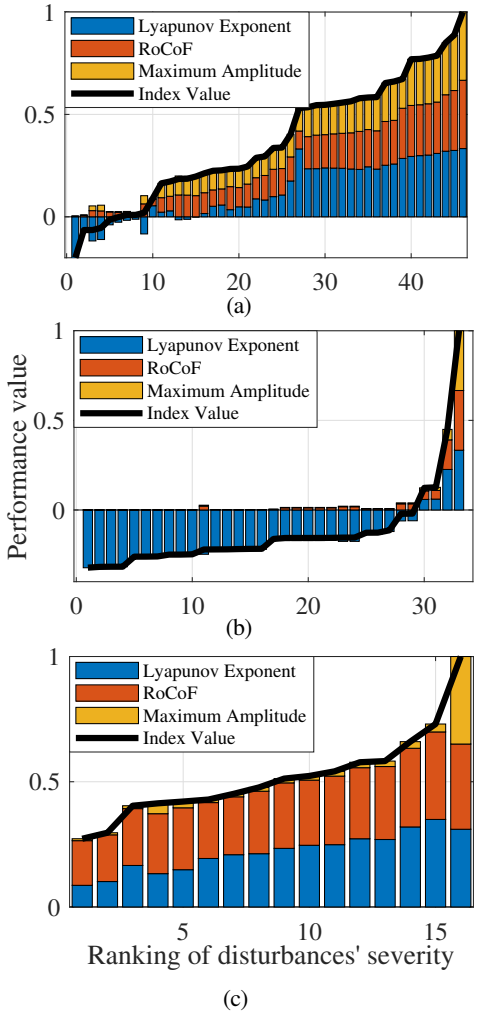

Fig. 4: Behavior of indices in the MIS without wind penetration. (a) Generator trips. (b) Line trips. (c) Load trips.

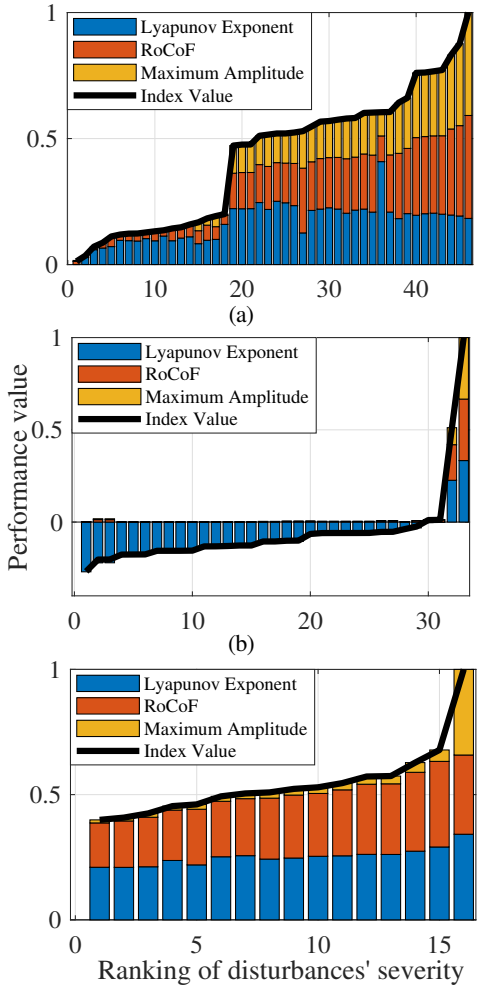

Fig. 5: Behavior of indices in the MIS with an 8.0% of wind penetration. (a) Generator trips. (b) Line trips. (c) Load trips.

A. *Generator trips*

In the case without wind generation, the severity indices in the presence of generator trips are depicted in Fig. 4a, displaying that the less severe disturbances correspond to generators 42, 15, 34, 33, 30 and 22. In all these disturbances, the Lyapunov exponent is negative, indicating that the stability is retained after their occurrences. Where the most severe disturbances are associated with generators 10, 3, 4, 2, and 5 (from less to the most severe). In contrast, in the case with wind generation, the evaluation of severity is presented in Fig. 5a, where the disconnection of G41 preserves the stability of the MIS. Notice that the system is generally unstable to generator trips, indicating an increment of severity in comparison with the case without wind generation.

B. *Line trips*

The ranking of severity for this type of disturbance occurring in the MIS without any renewable penetration is presented in Fig. 4b, showcasing a stable system response for 29 disturbances and unstable behavior for 4 disturbances. The less five severe disturbances are associated with the interconnections: 98-102 (Victoria-Nopala), 52-51 (Temascal-Tuxtla), 50-52 (Temascal-Tuxtla), 71-74 (Tecnologico-Tecnologico Potencia), 71-73 (Tecnologico-Tecnologico Cs1). All these transmission lines have a rated voltage of 400 kV [22]. Meanwhile, the ranking for the wind penetration case is exhibited in Fig. 5b, pointing out that the magnitude of the negative Lyapunov exponents decreases, and demonstrating that the disconnection of lines is more severe when the WPPs are integrated. Notice that 31 disturbances are stable in this case, being corroborated by the general index which exhibits that this type of disturbance is the less severe.

C. *Load trips*

When load trips take place across the MIS without wind penetration, the assessment of severity reports that all load disconnections lead to unstable system responses, as shown in Fig. 4c, where the severity index varies from 0.27 up to 1, indicating that this type of disturbance is the most severe in the MIS, since its stability is seriously affected. In contrast, when the MIS has WPPs, the ranking of severity illustrates a similar tendency, but the index value reaches higher values starting from 0.39 up to 1. So, these disturbances are the most severe in comparison with those associated with generators and transmission lines.

D. *General evaluation*

After assessing the severity of each disturbance separately, a general evaluation of 95 simulated disturbances is also carried out compiling all of them in Fig. 6. The ranking of severity for the MIS without wind penetration is depicted in Fig. 6a, where the less severe disturbances occur when the transmission lines disconnected correspond to the less loaded zones of the MIS, only 5 disturbances are not associated with generator trips. Likewise, the ranking for the case with wind integration is exhibited in Fig. 6b. It is remarkable that the magnitude of the performance value decreases, indicating the system's flexibility to disconnecting disturbances. Besides it can be observed that 70% of the disturbances are unstable in comparison with 60% when there are no WPPs.

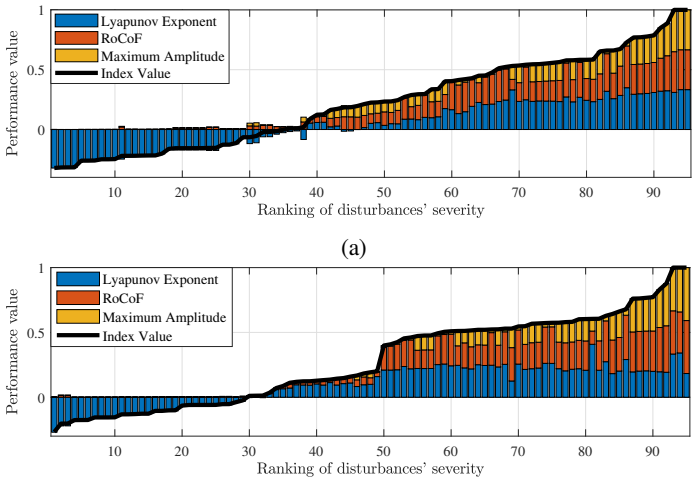

Fig. 6: Ranking of severity for all disturbances in the MIS. (a) Without wind generation

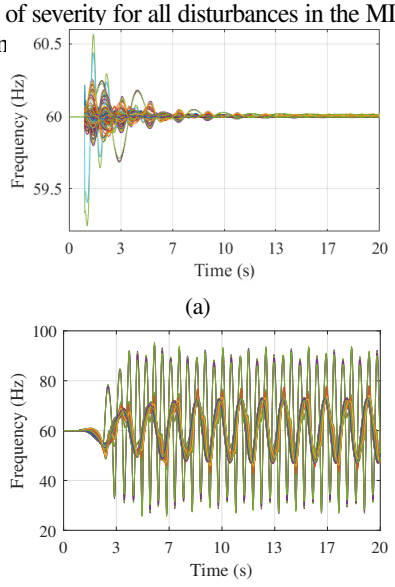

Fig. 7: Behavior of the simulated system response for: (a) the less severe disturbance; and (b) the worst severe disturbance.

The simulated system response for the MIS with wind generation, when two disturbances occur, is shown in Fig. 7. The less severe disturbance is displayed in Fig. 7a, noting momentary frequency excursions above 0.5Hz that effectively tend to return to the steady state in the 20s window analyzed. On the contrary, the worst severe disturbance is depicted in Fig. 7b, where it is evident the unstable behavior to the loss of ability for returning to the rated frequency value of 60Hz.

VI. Conclusions

This paper has demonstrated through the proposed methodology that is possible to assess and rank the disturbances' severity in large-scale power systems interfaced with WPPs, being helpful and useful to know the less and most severe disturbances in power grids. This is achieved by using quantification indices which represent patterns of the frequency behavior across the system. This implementation allowed the sorting of the selected disturbances and facilitated their analysis. Since the proposal has been evaluated using a percentage renewable penetration level, it can be useful for system operators when new power plants are interconnected.

According to the complete assessment of the disturbances' severity in the Mexican interconnected system, it is observed that 40% of the disturbances are stable when there are no WPPs interconnected. In contrast, when the system is interfaced with an 8% of wind generation, just 30% of the disturbances are stable. Thereby, Figures 4-5 allow inferring that disturbances associated with line trips are less severe since 88% of them are stables. On the contrary, the most severe disturbances correspond to the disconnection of loads, where 100% of them are unstable. Thus, all three indices demonstrate to be a reliable and robust measure to quantify the disturbances' severity and to analyze the stability in large-scale power systems to different operating conditions, penetration of RESs, and different type of disturbances.

Acknowledgment

M.R.A. Paternina acknowledges financial support from the Project Support Program for Research and Technological Innovation of UNAM (DGAPA, PAPIIT-2023-2025) through the project IT102723.

References

[1] A. R. Messina, *Wide area monitoring of interconnected power systems*. The Institution of Engineering and Technology, 2015.

[2] N. Khadka, R. Paudel, B. Adhikary, A. Bista, S. Sharma, and A. Shrestha, "Transient stability in renewable energy penetrated power systems: A review," 12 2020.

[3] S. Impram, S. Nese, and B. Oral, "Challenges of renewable energy penetration on power system flexibility: A survey," *Energy Strategy Reviews*, vol. 31, p. 100539, 09 2020.

[4] B. Mohandes, M. Moursi, N. Hatziargyriou, and S. Khatib, "A review of power system flexibility with high penetration of renewables," *IEEE Trans. Power Systems*, vol. Early access, pp. 1–13, 01 2019.

[5] N. Koltsaklis, A. Dagoumas, and I. Panapakidis, "Impact of the penetration of renewables on flexibility needs," *Energy Policy*, vol. 109, pp. 360–369, 10 2017.

[6] L. Shi, S. Sun, L. Yao, Y. Ni, and M. Bazargan, "Effects of wind generation intermittency and volatility on power system transient stability," *IET Renewable Power Generation*, vol. 8, no. 5, pp. 509–521, 2014.

[7] S. Savulescu, *Real-Time Stability in Power Systems: Techniques for Early Detection of the Risk of Blackout*, ser. Power Electronics and Power Systems. Springer International Publishing, 2014.

[8] *Power System Stability And Control*, ser. EPRI power system engineering series. McGraw-Hill, 1994.

[9] S. M. Rovnyak, M. N. Nilchi, D. W. Longbottom, and D. C. Vasquez, "Angle stability predictive indices," in *2012 IEEE Power and Energy Society General Meeting*, 2012, pp. 1–6.

[10] O. Gomez and M. Rios, "Interarea stability prediction index based on phasorial measurement," 01 2012.

[11] Y. Wu, L. Badesa, M. T. Musavi, and P. Lerley, "Monitoring power system transient stability using synchrophasor data," in *2015 IEEE Power Energy Society General Meeting*, 2015, pp. 1–5.

[12] N. Khadka, R. Paudel, B. Adhikary, A. Bista, S. Sharma, and A. Shrestha, "Transient stability in renewable energy penetrated power systems: A review," 12 2020.

[13] C. Rüeger, J. Dobrowolski, P. Korba, and F. R. S. Sevilla, "Lyapunov exponent for evaluation and ranking of the severity of grid events on extra-large power systems," in *2019 IEEE PES Innovative Smart Grid Technologies Europe (ISGT-Europe)*, 2019, pp. 1–5.

[14] ——, "Stability effects after massive integration of renewable energy sources on extra-large power systems," in *2020 IEEE PES Transmission Distribution Conference and Exhibition - Latin America (TD LA)*, 2020, pp. 1–6.

[15] B. Kharabian and H. Mirinejad, "Fuzzy Lyapunov exponents placement for chaos stabilization," *Physica D Nonlinear Phenomena*, vol. 445, p. 133648, Mar. 2023.

[16] H. Khodadadi and et al, "Applying a modified version of lyapunov exponent for cancer diagnosis in biomedical images: the case of breast mammograms," *Multidimensional Systems and Signal Processing*, vol. 29, 01 2018.

[17] H. Verdejo, L. Vargas, and W. Kliemann, "Stability of linear stochastic systems via lyapunov exponents and applications to power systems," *Applied Mathematics and Computation*, vol. 218, p. 11021–11032, 07 2012.

[18] ——, "Linear stability via lyapunov exponents in electrical power systems," *Latin America Trans., IEEE (Revista IEEE America Latina)*, vol. 11, pp. 1332–1337, 12 2013.

[19] M. Amiri, M. Dehghani, A. Khayatian, and M. Mohammadi, "Lyapunov exponent based stability assessment of power systems," 10 2019, pp. 1–5.

[20] K. Yoon, D. Choi, S. H. Lee, and J.-W. Park, "Optimal placement algorithm of multiple dgs based on model-free lyapunov exponent estimation," *IEEE Access*, vol. PP, pp. 1–1, 07 2020.

[21] S. Wei, M. Yang, J. Qi, J. Wang, S. Ma, and X. Han, "Model-free mle estimation for online rotor angle stability assessment with pmu data," *IEEE Trans. Power Systems*, vol. PP, 05 2018.

[22] CENACE, *Public Information about the Mexican Interconnected System*, 2023(accessed May 9, 2023), https://github.com/64josemanuel/mexicansystem.git.

[23] C. Pickover, "Visualizing chaos: Lyapunov surfaces and volumes," *IEEE Computer Graphics and Applications*, vol. 10, no. 2, pp. 15–19, 1990.

[24] J. H. Chow, K. Cheung, and R. Graham, "Power system toolbox webpage," 1990, [Web; accedido el 21-04-2023]. [Online]. Available: URL{https://sites.ecse.rpi.edu/~chowj/PST_2020_Aug_10.zip}

[25] P. W. Sauer *et al.*, *Power system dynamics and stability with Synchrophasor Measurement and Power System Toolbox, second edition*. John Wiley & Sons, 2017.

[26] I. M. Dudurych, "The impact of renewables on operational security: Operating power systems that have extremely high penetrations of nonsynchronous renewable sources," *IEEE Power and Energy Magazine*, vol. 19, no. 2, pp. 37–45, 2021.

[27] J. Holzfuss and U. Parlitz, *Lyapunov exponents from time series*, 11 2006, vol. 915, pp. 263–270.

[28] H. Bosetti and S. Khan, "Transient stability in oscillating multi-machine systems using lyapunov vectors," *IEEE Trans. Power Systems*, vol. 33, no. 2, pp. 2078–2086, 2018.

[29] S. Dasgupta, M. Paramasivam, U. Vaidya, and V. Ajjarapu, "Real-time monitoring of short-term voltage stability using pmu data," *IEEE Trans. Power Systems*, vol. 28, no. 4, pp. 3702–3711, 2013.

[30] "Ieee standard for synchrophasor measurements for power systems," *IEEE Std C37.118.1-2011 (Revision of IEEE Std C37.118-2005)*, pp. 1–61, Dec 2011.

[31] IEEE, "IEEE Standard for Synchrophasor Measurements for Power Systems – Amendment 1: Modification of Selected Performance Requirements," *IEEE Std C37.118.1a-2014 (Amendment to IEEE Std C37.118.1-2011)*, pp. 1–25, April 2014.

[32] A. Messina, J. Ramirez, and J. Canedo C., "An investigation on the use of power system stabilizers for damping inter-area oscillations in longitudinal power systems," *IEEE Trans. Power Systems*, vol. 13, no. 2, pp. 552–559, 1998.

[33] M. R. A. Paternina, J. M. Ramirez-Arredondo, J. D. Lara-Jiménez, and A. Zamora-Mendez, "Dynamic equivalents by modal decomposition of tie-line active power flows," *IEEE Trans. Power Systems*, vol. 32, no. 2, pp. 1304–1314, 2017.